Journal of Power Sources 195 (2010) 3494–3497

Contents lists available at ScienceDirect

Journal of Power Sources

journal homepage: www.elsevier.com/locate/jpowsour

Short communication

Thin film solid oxide fuel cells with copper cermet anodes

Zhongliang Zhan [a,b,*], Shung Ik Lee [b]

[a] Shanghai Institute of Ceramics, Chinese Academy of Sciences, 1295 Ding-Xi Road, Shanghai 200050, PR China
[b] Franklin Fuel Cells, 320 Circle of Progress, Suite 102, Pottstown, PA 19464, United States

ARTICLE INFO

Article history:
Received 19 November 2009
Received in revised form 2 December 2009
Accepted 3 December 2009
Available online 29 December 2009

Keywords:
Cathode-supported solid oxide fuel cells
Copper cermet anode
Tape casting
Infiltration

ABSTRACT

Thin film solid oxide fuel cells (SOFCs), composed of thin coatings of 8 mol% Y_2O_3-stabilized ZrO_2 (YSZ) and thick substrates of $(La_{0.8}Sr_{0.2})_{0.98}MnO_3$ (LSM)–YSZ cathodes, are fabricated using the conventional tape casting and tape lamination techniques. Densification of YSZ electrolyte thin films is achieved at 1275 °C by adjusting the cathode tape formulation and sintering characteristics. Two types of copper cermets, CuO–YSZ–ceria and CuO–SDC ($Ce_{0.85}Sm_{0.15}O_{1.925}$)–ceria, are compared in terms of the anodic performance in hydrogen and propane. Maximum power densities for hydrogen and propane at 800 °C are 0.26 W cm^{-2} and 0.17 W cm^{-2} for CuO–YSZ–ceria anodes and 0.35 W cm^{-2} and 0.22 W cm^{-2} for CuO–SDC–ceria anodes, respectively. Electrochemical impedance analysis suggests that CuO–SDC–ceria exhibits a much lower anodic polarization resistance than CuO–YSZ–ceria, which could be explained by the intrinsic mixed oxygen ionic and electronic conductivities for SDC in the reducing atmosphere.

1. Introduction

Significant efforts have been undertaken to promote the development of direct hydrocarbon solid oxide fuel cells (SOFCs) due to the advantages of simplified system design and improved system efficiency. Nonetheless, direct exposure of hydrocarbon fuels to the conventional nickel based anodes has been problematic due to their high catalysis for hydrocarbon cracking reactions at the operating temperatures, leading to carbon accumulation in the anode and thus eventually degrading the cell performance [1]. Alternative anode materials with little or no nickel and with significantly reduced catalysis for coking formation reactions were thus developed such as copper–ceria–YSZ [2], lanthanum strontium titanate [3], lanthanum strontium chromites doped with manganese [4,5] or ruthenium [6], and $Sr_2Mg_{1-x}Mn_xMoO_{6-\delta}$ [7]. The Cu/YSZ/CeO_2 anodes were particularly effective for the direct use of varieties of heavy hydrocarbon fuels, *e.g.*, butane and decane, and exhibited substantially enhanced resistance to deactivation from carbon deposition and sulfur poisoning [2]. The success of the copper anode system could be ascribed to the low susceptibility for coking of copper, appearing to only provide electrical conduction, and reasonably high catalytic activity of ceria for fuel oxidation due to its intrinsic mixed ionic and electronic conducting behaviour in reducing atmosphere.

Low melting points of copper oxides (1235 °C for Cu_2O and 1326 °C for CuO) make direct co-sintering of the anodes and the electrolytes infeasible, which is nonetheless necessary for densification of electrolyte thin films and has been typically used for the conventional nickel anode system. Up to date, the copper cermet anodes have been fabricated using a unique two-step process, consisting of formation of porous YSZ skeleton on the electrolyte using the conventional ceramic technique and addition of copper oxide and ceria by impregnation of nitrate solutions and calcinations [8]. While such an impregnation process allows unprecedented control over composition and microstructure, the multiple cycles of impregnation and calcinations, as required to achieve a continuous copper network for sufficient electron conduction and enough amounts of ceria for catalysis, may prevent the practical implementation of the infiltration approach.

In this paper, cathode-supported SOFCs were fabricated using conventional tape tasting and tape lamination techniques, whereas the CuO–YSZ cermet anodes were applied to the electrolyte through screen-printing and low temperature calcination, thus avoiding evaporation and melting of copper oxides. This new approach allowed a high loading of copper in the cermets that otherwise could not be easily achieved by multiple impregnation and calcinations. Previous reports showed that ceria was critical in enhancing the anodic reactions in SOFCs [9], the copper cermets were thus further impregnated with aqueous solutions of $Ce(NO_3)_3$ followed by calcinations at 450 °C, yielding approximately 10% of ceria in the anodes. Since the anode layer was typically thin (≈50 μm) and ceria loading was relatively low (10%), the impregnation process could be finished within one or two cycles. The electrochemical characteristics of these cells were evaluated in hydrogen and propane.

* Corresponding author at: Shanghai Institute of Ceramics, Chinese, Academy of Sciences, Research Center of Energy Conversion Materials, 1295 Ding-Xi Road, Shanghai 200050, PR China. Tel.: +86 21 5241 2191; fax: +86 21 5241 3903.
E-mail addresses: zhongliangzhan@gmail.com, zzhan@mail.sic.ac.cn (Z. Zhan).

0378-7753/$ – see front matter © 2009 Elsevier B.V. All rights reserved.
doi:10.1016/j.jpowsour.2009.12.017

2. Experimental procedures

Thin film SOFCs with thick cathode supports were fabricated using the conventional organic tape casting and tape lamination techniques. The cathode powders of LSM ($(La_{0.8}Sr_{0.2})_{0.98}MnO_3$, 7 $m^2\,g^{-1}$, Praxair), YSZ (TZ-8YS, 7 $m^2\,g^{-1}$, Tosoh) and rice starch (Sigma–Aldrich) in a weight ratio of 40:40:20 were ball-milled for 24 h with appropriate amounts of dispersant, binder, plasticizer and solvent. The resulting homogeneous slurry was then cast under the doctor blade. After drying, green LSM–YSZ cathode sheets of ≈200 μm thick were obtained. Similarly, green YSZ electrolyte sheets of ≈20 μm thick were prepared by casting YSZ slurry that was formed in the same way as in the case of LSM–YSZ except that no pore former was added. Two sheets of LSM–YSZ and one sheet of YSZ were then stacked and iso-statically laminated at 70 °C for 10 min under a pressure of 3000 psi, which were then co-sintered at 1275 °C for 4 h in order to densify the electrolyte layer. The pore size distributions of the cathode substrates were measured by mercury intrusion porosimetry (Micromeritics Instrument Corp., Norcross, GA) over a pressure range of 0.8–50,000 psi.

The copper anodes were prepared by mixing CuO powder (Alfa), YSZ or SDC ($Ce_{0.85}Sm_{0.15}O_{1.925}$, 7 $m^2\,g^{-1}$, Praxair) powder and rice starch in a weight ratio of 45:45:10. A screen-printing vehicle (Electro-Science Laboratory) was added to the mixed powder to make a slurry. The slurry was applied onto the YSZ electrolyte coating of half-cells by screen-printing and fired at 900 °C for 4 h. The copper anodes were further impregnated with aqueous solutions of $Ce(NO_3)_3$, subsequently calcined at 450 °C to form ceria. The quantity of the deposited ceria was estimated by weight difference and the final anode composition was 45–45–10 wt (CuO–YSZ/SDC–CeO_2) after two cycles of impregnation and calcinations. The microstructure of the cathode-supported SOFCs was examined using the scanning electron microscopy (JSM6390LV, JEOL).

For fuel cell tests, the anode sides of the cells were sealed to alumina tubes using a ceramic adhesive (Aremco, Ultra-Temp 552). Au and Ag current collectors were painted on the anode and cathode sides, respectively. Single SOFCs were tested in a tube furnace at temperatures from 700 °C to 800 °C, using hydrogen or propane as the fuel. Ambient air was maintained on the cathode side. Electrochemical impedances were measured using a Gamry Instruments Model EIS300 impedance spectrometer with a frequency range from 0.1 Hz to 100 kHz. Extrapolations of these spectra to the real axis were conducted to obtain the ohmic resistances as well as the total polarizations.

3. Results and discussion

Densification of electrolyte thin films at low temperatures is critically important for cathode-supported SOFCs to deliver reasonably high power densities due to the increasing susceptibility of the chemical reactions with temperature between lanthanum manganites and zirconia to form a secondary phase, $La_2Zr_2O_7$ [10]. The sintering characteristics of the cathode was tailored by altering the amounts of organic components in the green tapes to be compatible with that of the electrolyte tapes, producing flat half-cells with no warpage or delamination. A representative cross-sectional SEM image of the cathode-supported SOFCs was shown in Fig. 1. Even though the bi-layers of the cathode and electrolyte were co-sintered at 1275 °C, much lower than typically used sintering temperatures of 1350–1400 °C for the state-of-the-art nickel anode supported SOFCs, a crack-free, uniform and dense thin film of YSZ electrolyte was obtained. Densification of the supported electrolyte thin films at relatively low temperatures could be explained by the sintering dominance of the thick supporting cathode substrates, thus yielding relatively large linear shrinkage [11]. The overall shrinkage of these cells co-fired at 1275 °C was typically around 17.9%. The thickness of the electrolyte was approximately 15 μm and the bonding between the cathode substrate and the electrolyte was quite good. Fig. 1 also shows typical porous microstructure of the electrodes, as required to achieve adequate diffusion of fuel/oxygen to the electrochemically active triple phase boundaries (TPB). The estimated porosities were 40% and 35% for the Cu–YSZ–CeO_2 anode and the LSM–YSZ cathode, respectively. The mercury porosimetry measurement further confirmed that the cathode supports had an effective pore structure with the median pore size close to 2 μm, in good agreement with SEM observations.

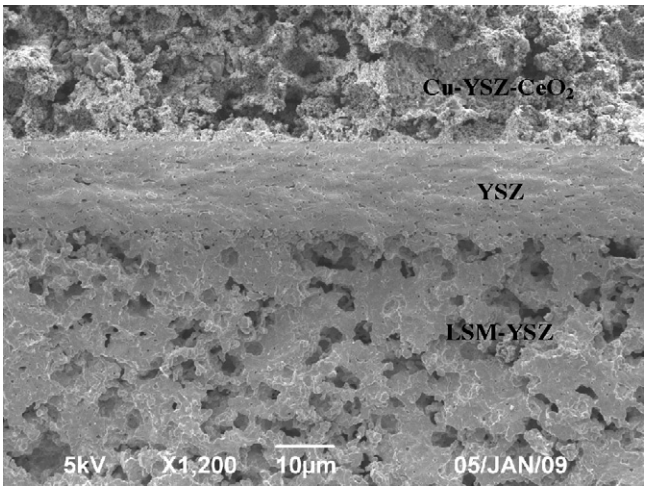

Fig. 1. Cross-sectional SEM image of the cathode-supported SOFCs (LSM–YSZ|YSZ|CuO–YSZ–CeO_2).

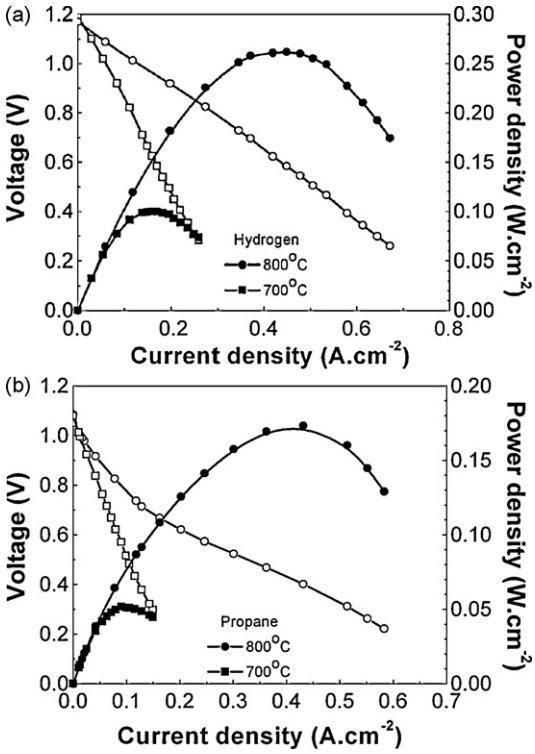

Fig. 2. Voltage and power density versus current density at 800 °C and 700 °C for the cells, LSM–YSZ|YSZ|CuO–YSZ–CeO_2, tested with (a) hydrogen at 60 sccm and (b) propane at 20 sccm in the anode and ambient air in the cathode.

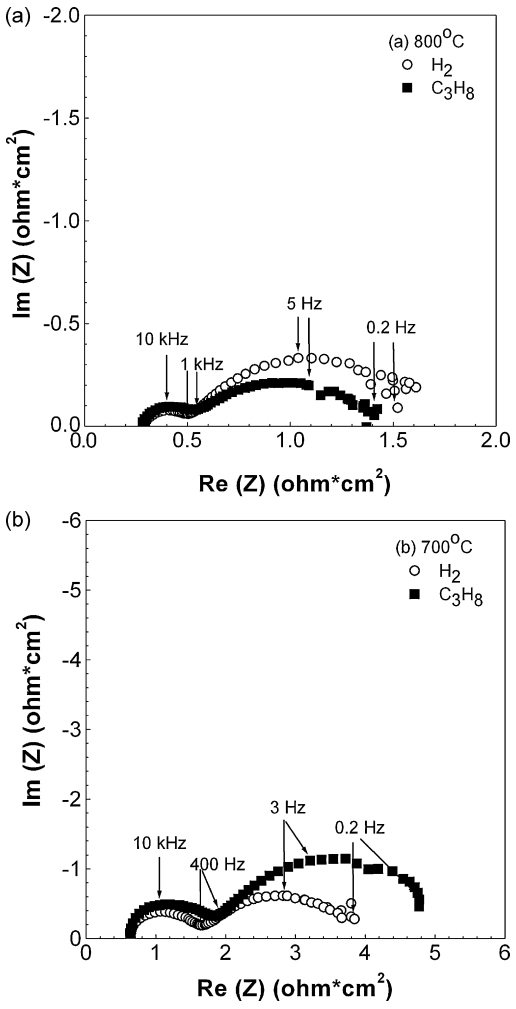

Fig. 3. Nyquist plots of the electrochemical impedance spectroscopy results from these cells: LSM–YSZ|YSZ|CuO–YSZ–CeO_2, at (a) high and (b) low temperatures. Each plot compares these cells in hydrogen at 60 sccm and propane at 20 sccm.

Fig. 2 shows the voltage V and power density P versus the current density J for the cathode-supported SOFCs with CuO–YSZ–CeO_2 anodes in (a) hydrogen and (b) propane at 700 °C and 800 °C. The terminal voltage of these cells in hydrogen exhibited a linear decrease with increasing current densities, yielding area specific resistance (ASR) values of 1.4 Ω cm^2 at 800 °C and 3.6 Ω cm^2 at 700 °C, respectively. In contrast, the cell polarization curve in propane at 800 °C featured a sharp decrease in terminal voltage for $J < 0.1$ A cm^{-2} and a gradual linear drop for $J > 0.2$ A cm^{-2}, which were, respectively dominated by the activation polarization and ohmic polarization. The estimated ASR values were 3.1 Ω cm^2 for $J < 0.1$ A cm^{-2} and 1.3 Ω cm^2 for $J > 0.2$ A cm^{-2}. Comparison of these ASR values suggested that the Cu–YSZ–ceria anodes had higher catalytic activity for the electrochemical oxidation of hydrogen than for that of propane. The maximum power densities were thus higher in hydrogen than in propane, *e.g.*, 0.26 W cm^{-2} for hydrogen versus 0.17 W cm^{-2} for propane at 800 °C.

Fig. 3 compares the electrochemical impedance spectra from cathode-supported SOFCs operated on hydrogen and propane at 800 °C and 700 °C. Note that the impedance in propane was collected under high polarizations in order to reduce the risk of coking formation. Overall, the Nyquist plots consisted of a small higher frequency depressed arc and a large lower frequency arc, both of which increased with decreasing temperature, as typically observed for the electrochemical processes such as charge transfer or surface diffusion. The pure ohmic resistance values, which were unaffected by the type of fuels in the anode, were 0.3 Ω cm^2 and 0.6 Ω cm^2 at 800 °C and 700 °C, respectively. The total ASR values were, respectively 1.4–1.5 Ω cm^2 and 3.8–4.8 Ω cm^2 at 800 °C and 700 °C, corresponding reasonably well with the slopes of the V–J curves as shown in Fig. 2.

The pure ohmic resistance was significantly higher than the value calculated for an electrolyte thin film of 15 μm thick using the measured ionic conductivity of 0.026 S cm^{-1} for YSZ at 800 °C, as previously observed [12]. This difference could be explained by a sharp drop in the electrical conductivity of the thick LSM–YSZ cathode substrates fired at 1275 °C due to the formation of a much less oxygen ionic conductor, *i.e.*, $La_2Zr_2O_7$, from the high temperature reaction between YSZ and LSM, even though a slight A-site deficiency like $(La_{0.8}Sr_{0.2})_{0.98}MnO_3$ might help prevent the formation of the pyrochlore phase even at 1400 °C [13]. The electrical conductivities of the porous LSM–YSZ substrates fired at 1275 °C, measured using the four-probe method, were only 0.1 S cm^{-1} and 0.2 S cm^{-1} at 700 °C and 800 °C, respectively. These values were approximately one order of magnitude lower than the conductivities (~4 S cm^{-1}) for the LSM–YSZ substrates fired at 1150 °C, where the electrical conduction was mainly through the LSM phase with an activation energy of ~0.1 eV [14]. The activation energy for the electrical conduction of LSM–YSZ cathode substrates fired at 1275 °C was calculated to be around 0.6 eV, indicative of a substantially increased contribution from the oxygen ionic conducting phases of YSZ and $La_2Zr_2O_7$ to the overall electrical conductivities.

In order to determine the respective contributions of the anode and the cathode to the overall electrode polarization resistance, electrolyte supported SOFCs with LSM–YSZ cathodes fired at 1150 °C and CuO–YSZ anodes impregnated with 10% CeO_2 were fabricated and analyzed using ac impedance. Total electrode polarization resistances of ≈0.9 Ω cm^2 were observed at 800 °C for these cells with the anode and the cathode exposed to hydrogen and air, respectively. By subtracting the polarization resistance from the LSM–YSZ cathode ($R_{LSM-YSZ-1150}$) fired at 1150 °C, which was calculated to be ≈0.2 Ω cm^2 at 800 °C from the impedance spectroscopy of the symmetric cathodes supported on the electrolytes, the polarization resistance from Cu–YSZ–ceria ($R_{Cu-YSZ-ceria}$) was calculated to be around ≈0.7 Ω cm^2. Similarly, the polarization resistance from the LSM–YSZ cathode supports was thus obtained by using the impedance shown in Fig. 3a: $R_{LSM-YSZ-1275} = 0.5$ Ω cm^2, much higher than 0.2 Ω cm^2 observed for LSM–YSZ cathodes fired at 1150 °C. These results suggest that the LSM–YSZ cathodes fired at 1275 °C, as used in these thin film SOFCs with copper anodes, had pronouncedly reduced catalytic activity for oxygen reduction reactions. One possible explanation was due to the formation of $La_2Zr_2O_7$ within the electrochemical reactive zones. Additionally, excessive coarsening of LSM particles as experimentally observed at high temperatures would result in a dramatic reduction in the triple phase boundaries for cathodic reactions since the TPB length in an electrode is inversely proportional to the grain size.

The above analysis indicated that the pure ohmic polarization, the anode and the cathode polarization were, respectively 0.3 Ω cm^2, 0.7 Ω cm^2 and 0.5 Ω cm^2 when the cathode-supported SOFCs with CuO–YSZ–ceria anodes were operated on hydrogen at 800 °C. Prior studies indicated that use of doped ceria as interfacial layers between anodes and electrolytes or as components in the anodes could remarkably reduce the anodic polarization losses [15,16]. In order to enhance the anodic catalysis for fuel oxidation, samarium doped ceria (SDC) was used to replace the pure ionic conducting phase (YSZ) in the above copper anodes. Fig. 4a shows the voltage V and power density P versus the current density J for the cathode-supported SOFCs with CuO–SDC anodes impregnated with 10% ceria operating on hydrogen and propane at 800 °C. The maximum power densities were 0.35 W cm^{-2} and 0.22 W cm^{-2} for

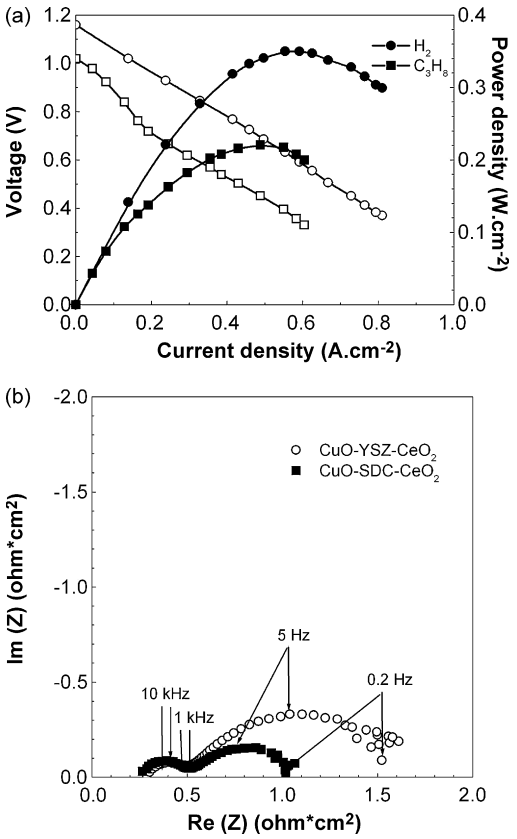

Fig. 4. Electrochemical characteristics at 800 °C for cathode-supported SOFCs, LSM–YSZ|YSZ|CuO–SDC–CeO_2: (a) voltage and power density versus current density for hydrogen and propane and (b) Nyquist plot of the electrochemical impedance spectroscopy for hydrogen. For comparison, the impedance for the cells with CuO–YSZ–ceria anodes was included.

hydrogen and propane, respectively. These values were approximately 30% higher than obtained with CuO–YSZ–ceria anodes. Fig. 4b compares the electrochemical impedance spectra for the cathode-supported SOFCs with Cu–YSZ–ceria and Cu–SDC–ceria anodes operated in hydrogen at 800 °C. The calculated anodic polarization resistance for Cu–SDC–ceria composites was around 0.2 Ω cm^2 at 800 °C, significantly lower than 0.7 Ω cm^2 for the Cu–YSZ–ceria anodes. Note that doped ceria usually exhibit mixed oxygen ionic and electronic conductive behaviour due to the susceptibility of partial reduction of Ce(IV) to Ce(III), especially in the reducing atmosphere. As an example, equal ionic and electronic conductivities of 0.08 S cm^{-1} were observed for doped ceria at 800 °C when exposed to a reducing atmosphere with oxygen partial pressure of 10^{-18} atm [17]. The enhanced catalysis from samarium doped ceria in the copper anodes for fuel oxidation reactions, as observed in Fig. 4b, was presumed to result from their intrinsic mixed oxygen ionic and electronic conducting characteristics in hydrogen, which allows a substantially enlarged electrochemical reaction zone from the conventional triple phase boundaries to the entire electrode/gas interface.

Besides high reproducibility, improved quality control and reduced cost of fabrication, the conventional ceramic processing of copper cermet anodes offers additional advantages in comparison with the approach of intensive infiltrations and calcinations. Firstly, high copper oxide loading could be easily acquired by simply altering the composition of the initial oxide mixtures. In contrast, progressive infiltration becomes increasingly difficult due to continuously reduced porosity, thus limiting the maximum amount of copper oxide formed through impregnation and calcinations. Secondly, the porous microstructure could be finely tailored by controlling the initial particle sizes of the oxide powders and fugitive materials. The three-dimensional distribution of copper oxide in the anodes might help suppress the coarsening of copper at operating temperatures, thus improving the long-term stability of the anode microstructure and performance. Most of the above electrochemical tests were conducted over 10–30 h, but a few long-term tests showed that the cathode-supported SOFCs with Cu–YSZ–ceria anodes could provide stable power densities in hydrogen over 500 h, *e.g.*, 0.2 W cm^{-2} at 0.5 V and 800 °C.

4. Summary and conclusions

In summary, we have successfully fabricated the LSM–YSZ cathode-supported SOFCs with copper anodes using the conventional ceramic processing technology. Maximum power densities for these cells with CuO–YSZ–ceria anodes at 800 °C were 0.26 W cm^{-2} and 0.17 W cm^{-2} in hydrogen and propane, respectively. The substitution of SDC, a mixed ionic and electronic conductor, for YSZ in the copper anode resulted in increased maximum power densities, *e.g.*, 0.35 W cm^{-2} for hydrogen and 0.22 W cm^{-2} for propane. Impedance analysis revealed that the anodic polarization resistance for CuO–SDC–ceria in hydrogen was much lower than for CuO–YSZ–ceria, *e.g.*, 0.2 Ω cm^2 versus 0.7 Ω cm^2 at 800 °C. The relatively high cathodic polarization resistance of 0.5 Ω cm^2 at 800 °C in the LSM–YSZ cathode-supported SOFCs suggests that it is critically important to optimize the chemical composition and porous microstructure of the cathode substrates in order to further improve the cell performance.

References

[1] S.A. Barnett, in: W. Vielstich, A. Lamm, H. Gasteiger (Eds.), Handbook of Fuel Cells, vol. 4, Wiley, Hoboken, NJ, 2003, pp. 1098–1108.
[2] S.D. Park, J.M. Vohs, R.J. Gorte, Nature 404 (2000) 265–267.
[3] O.A. Marina, N.L. Canfield, J.W. Stevenson, Solid State Ionics 149 (2002) 21–28.
[4] J. Liu, B.D. Madsen, Z. Ji, S.A. Barnett, Electrochem. Solid-State Lett. 5 (6) (2002) A122–A124.
[5] S. Tao, J.T.S. Irvine, S.M. Plint, J. Phys. Chem. B 110 (2006) 21771–21776.
[6] B.D. Madsen, W. Kobsiriphat, Y. Wang, L.D. Marks, S.A. Barnett, J. Power Sources 166 (2007) 64–67.
[7] Y. Huang, R.I. Doss, Z. Xing, J.B. Goodenough, Science 312 (2006) 254–257.
[8] S. Jung, C. Lu, H. He, K. Ahn, R.J. Gorte, J.M. Vohs, J. Power Sources 154 (2006) 42–50.
[9] A. Atkinson, S. Barnett, R.J. Gorte, J.T.S. Irvine, A.J. Mcevoy, M. Mogensen, S.C. Singhal, J. Vohs, Nat. Mater. 3 (2004) 17–27.
[10] S.P. Jiang, J.G. Love, J.P. Zhang, M. Hoang, Y. Ramprakash, A.E. Hughes, S.P.S. Badwal, Solid State Ionics 121 (1999) 1–10.
[11] K. Yamahara, C.P. Jacobson, S.J. Visco, L.C.D. Jonghe, Solid State Ionics 176 (2005) 451–456.
[12] Y. Huang, J.M. Vohs, R.J. Gorte, J. Electrochem. Soc. 152 (7) (2005) A1347–A1353.
[13] L. Kindermann, D. Das, D. Bahadur, D. Bahadur, R. Weiß, H. Nickel, K. Hilpert, J. Am. Ceram. Soc. 80 (4) (1997) 909–914.
[14] T. Tsai, S.A. Barnett, Solid State Ionics 93 (1997) 207–217.
[15] T. Tsai, S.A. Barnett, Solid State Ionics 98 (1997) 191–196.
[16] H. Uchida, T. Osuga, M. Watanabe, J. Electrochem. Soc. 146 (5) (1999) 1677–1682.
[17] V.P. Gorelov, V.B. Balakireva, I.Y. Yaroslavtsev, V.A. Kazantsev, E.G. Vaganov, Russ. J. Electrochem. 43 (8) (2007) 935–941.